

SUPPORTING INFORMATION

Photophysical Studies of C,C'-Bis(benzodiazaborolyl)dicarba-*closos*-dodecaboranes.

Lothar Weber,*^a Jan Kahlert,^a Regina Brockhinke,^a Lena Böhling,^a Johannes Halama,^a Andreas Brockhinke,^a Hans-Georg Stammler,^a Beate Neumann,^a Carlo Nervi,^b Rachel A. Harder^c and Mark A. Fox^c

^a Fakultät für Chemie der Universität Bielefeld, 33615 Bielefeld, Germany

E-mail: lothar.weber@uni-bielefeld.de

^b Dipartimento di Chimica IFM, via P. Giuria 7, 10125 Torino, Italy

^c Department of Chemistry, Durham University, Durham DH1 3LE, United Kingdom

Contents

¹ H, ¹ H{ ¹¹ B}, ¹³ C and ¹¹ B{ ¹ H} NMR spectra figures for 16 - 21	S2-S13
Crystallographic data for 16 - 19, 21 and 23	S14
Additional photophysical data for 16 - 21	S15-S18
Experimental and simulated CV plots	S19-S21
Computational data	S22-S23

Figure S1: ^1H NMR spectrum of **16**

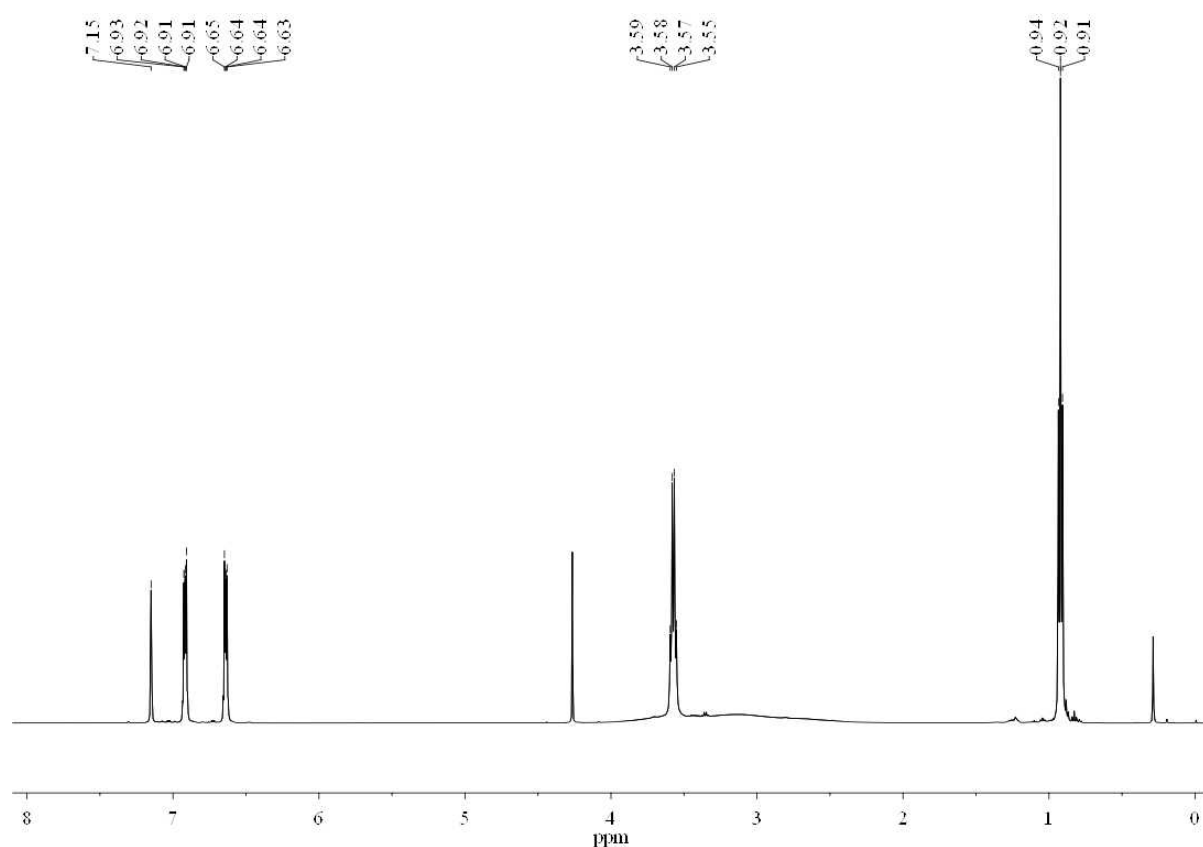


Figure S2: $^1\text{H}\{\text{B}^{11}\}$ NMR spectrum of **16**

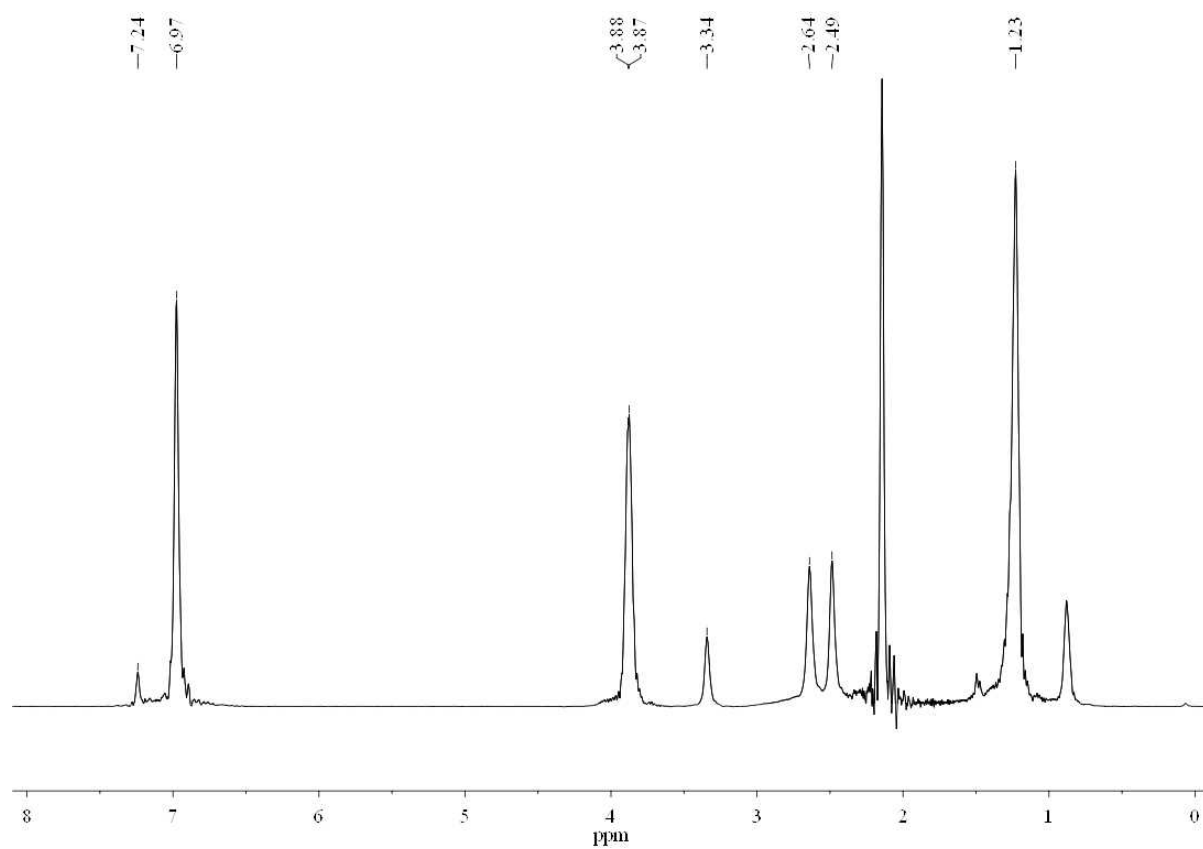


Figure S3: $^{13}\text{C}\{^1\text{H}\}$ NMR spectrum of **16**

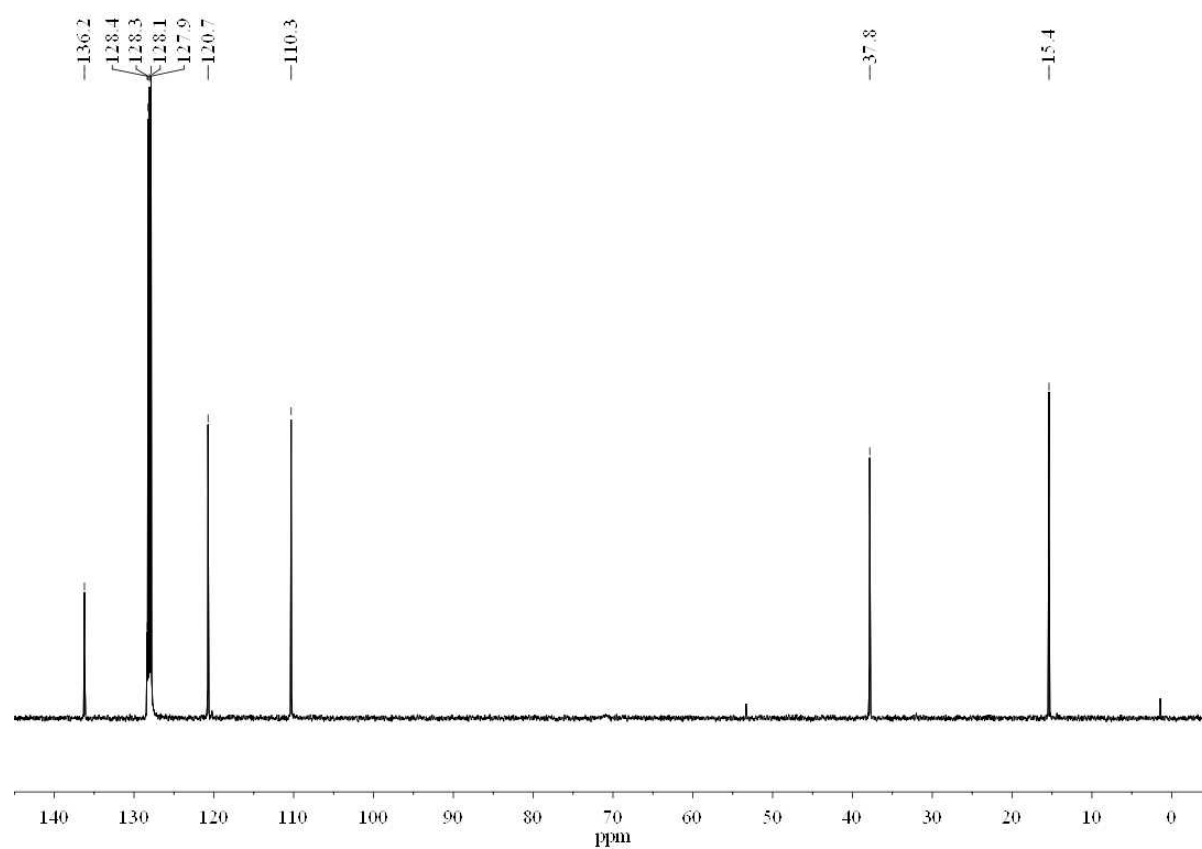


Figure S4: $^{11}\text{B}\{^1\text{H}\}$ NMR spectrum of **16**

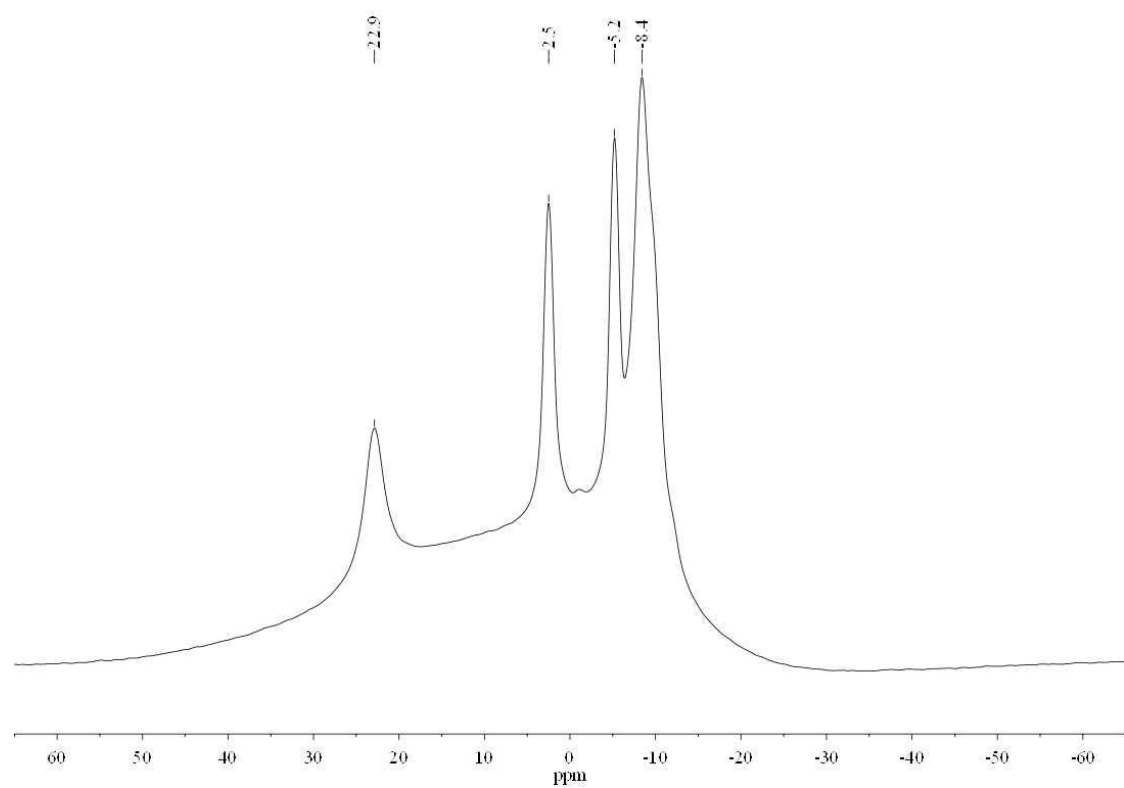


Figure S5: ^1H NMR spectrum of **17**

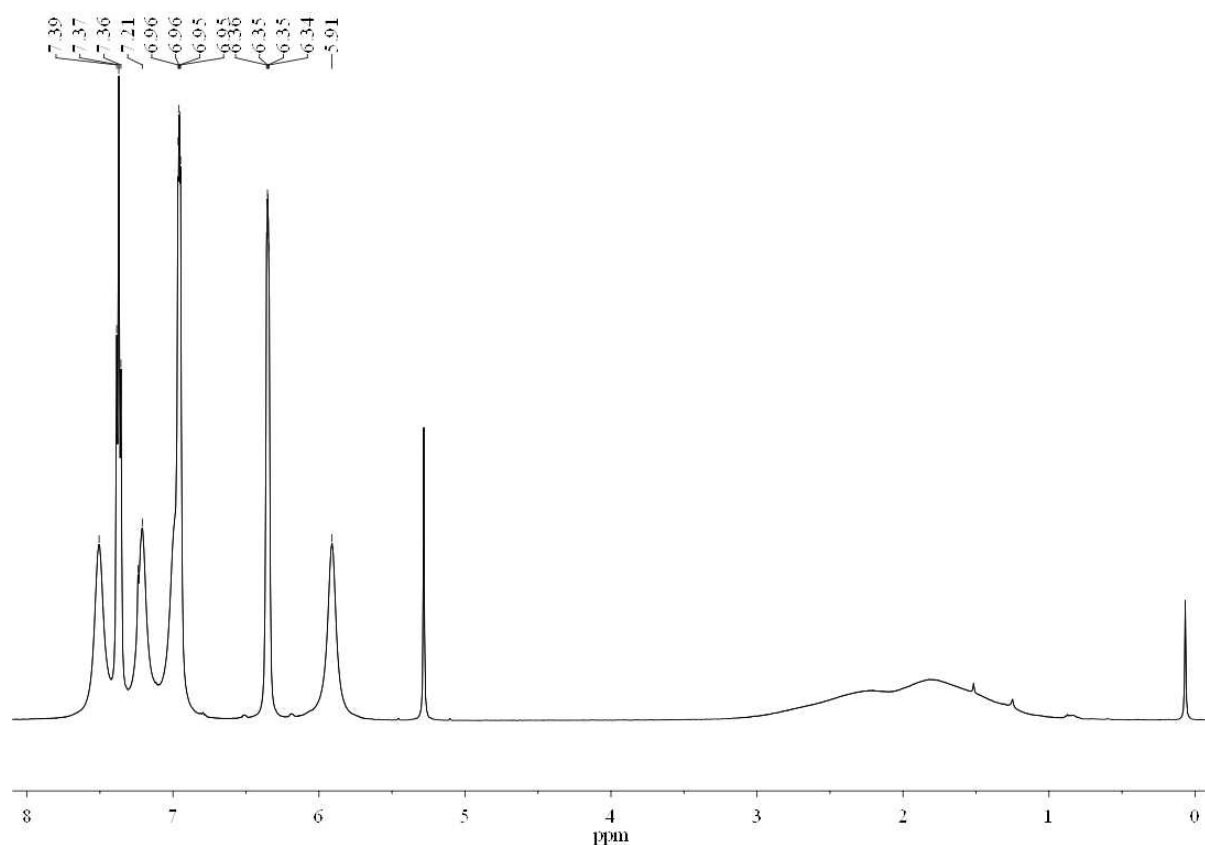


Figure S6: $^1\text{H}\{\text{B}^{11}\}$ NMR spectrum of **17**

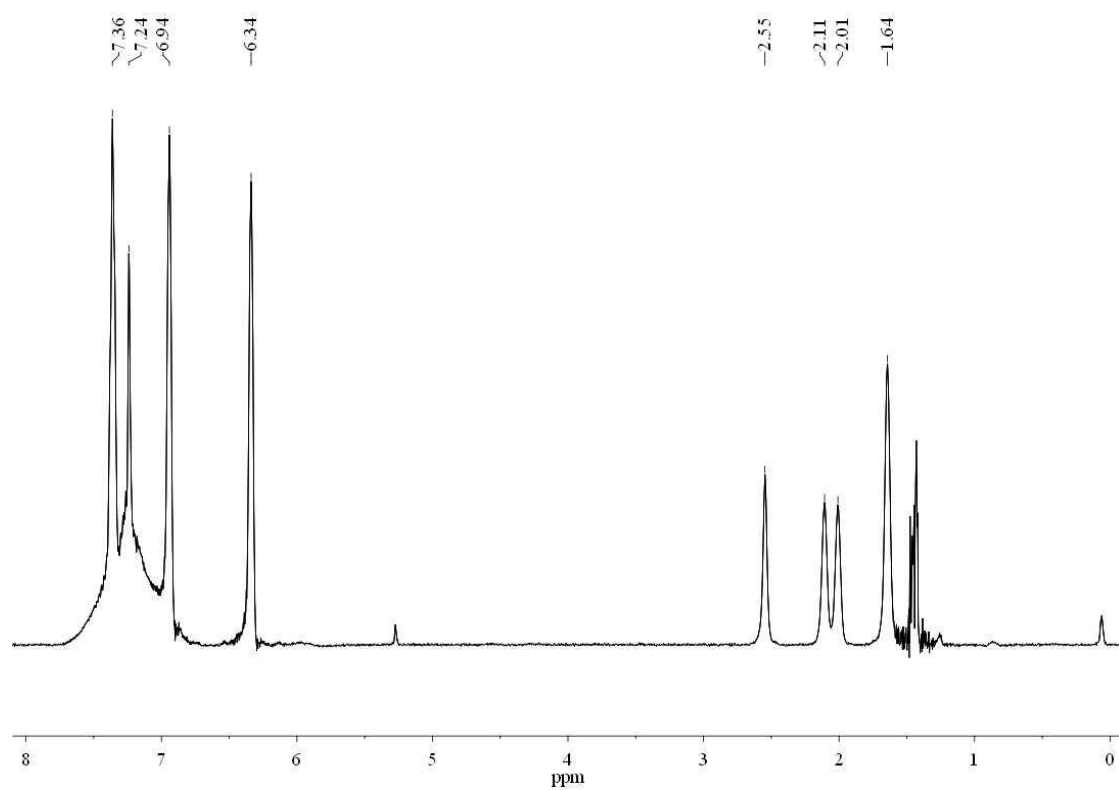


Figure S7: $^{13}\text{C}\{^1\text{H}\}$ NMR spectrum of **17**

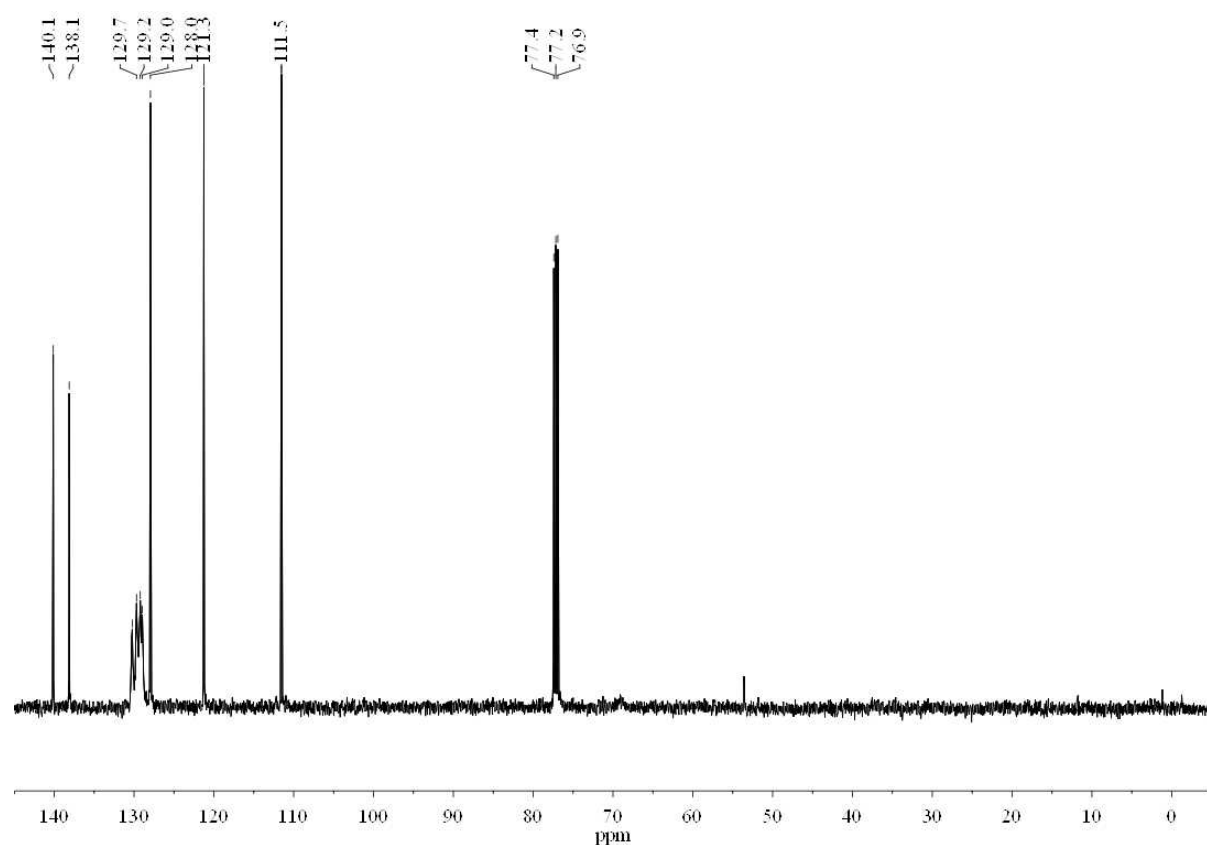


Figure S8: $^{11}\text{B}\{^1\text{H}\}$ NMR spectrum of **17**

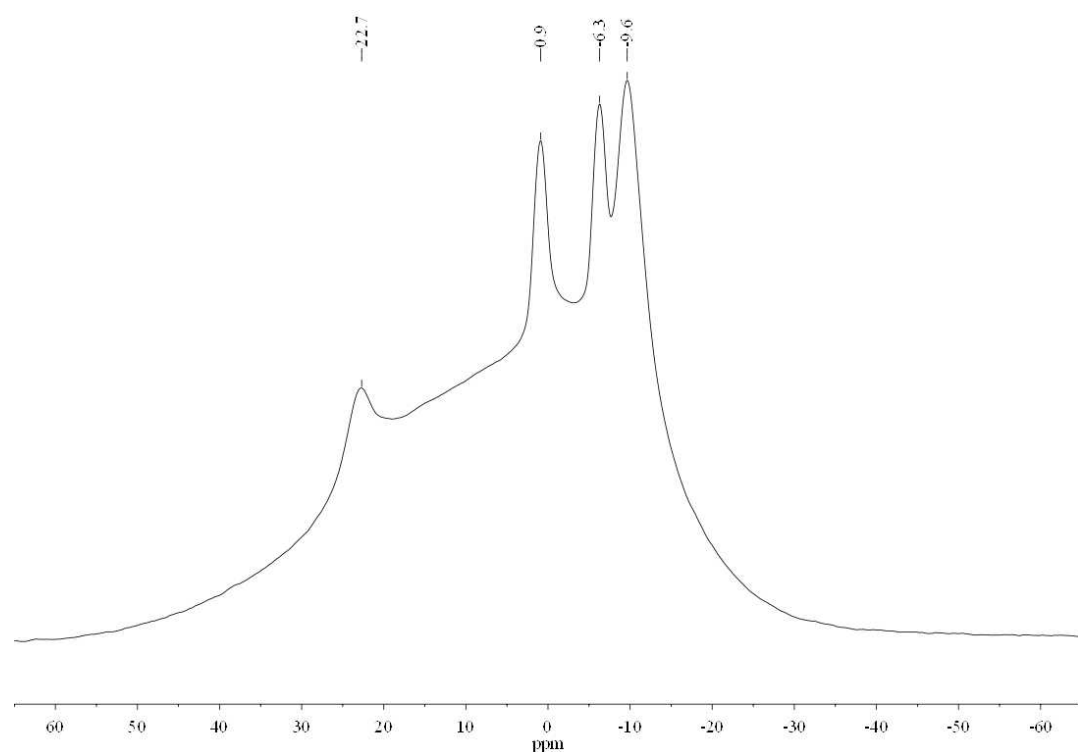


Figure S9: ^1H NMR spectrum of **18**

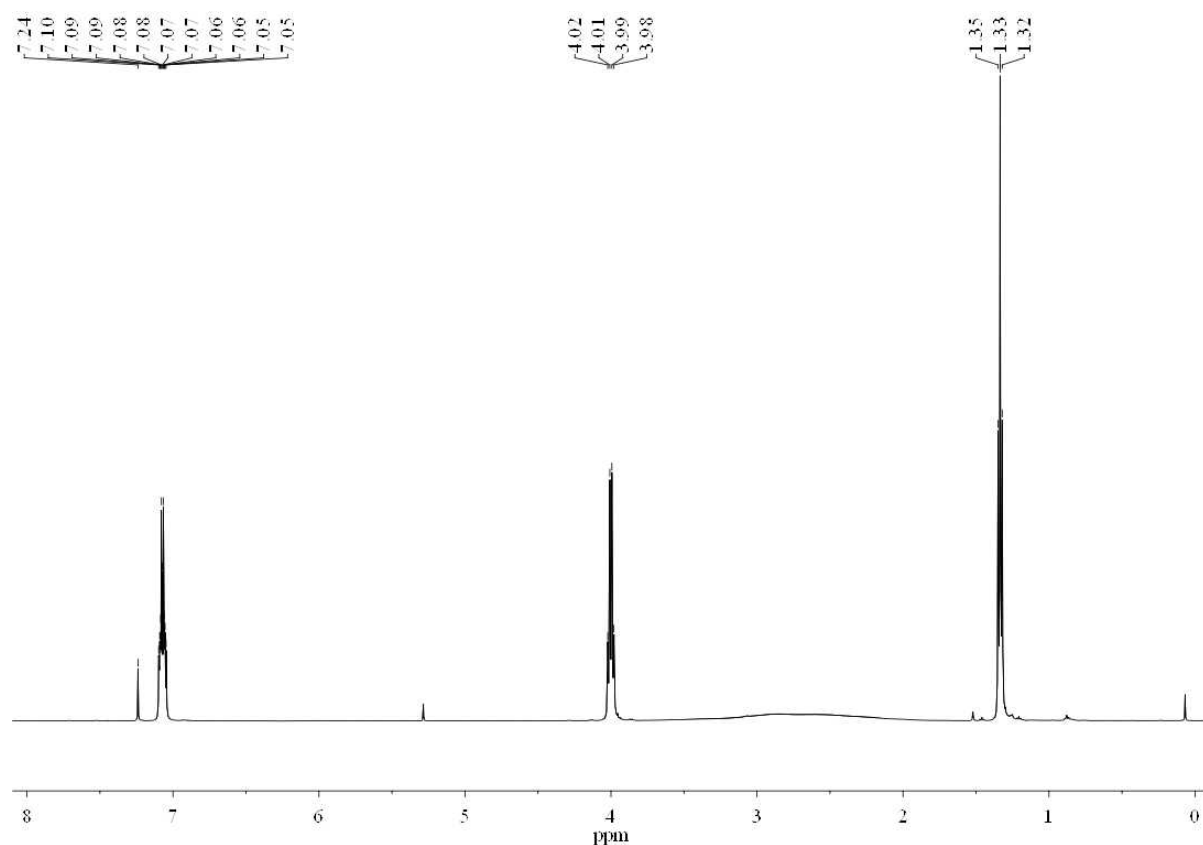


Figure S10: $^1\text{H}\{^{11}\text{B}\}$ NMR spectrum of **18**

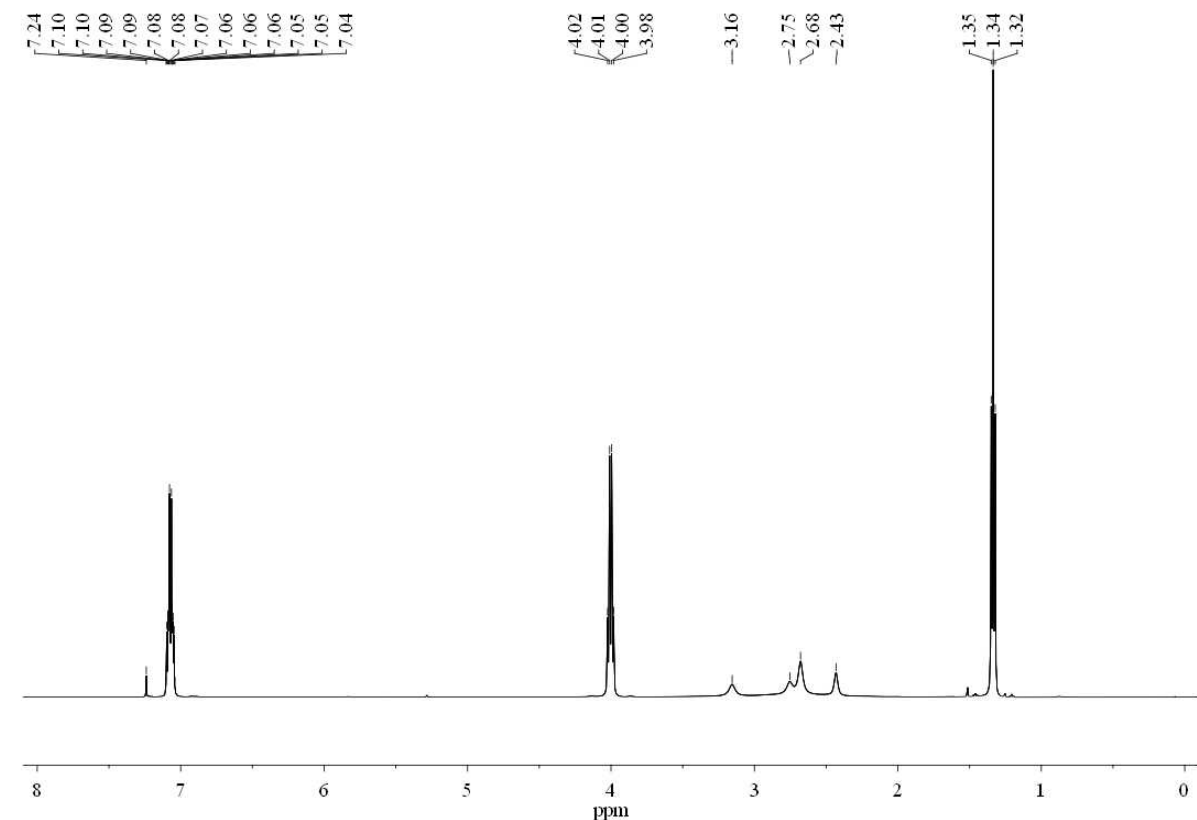


Figure S11: $^{13}\text{C}\{^1\text{H}\}$ NMR spectrum of **18**

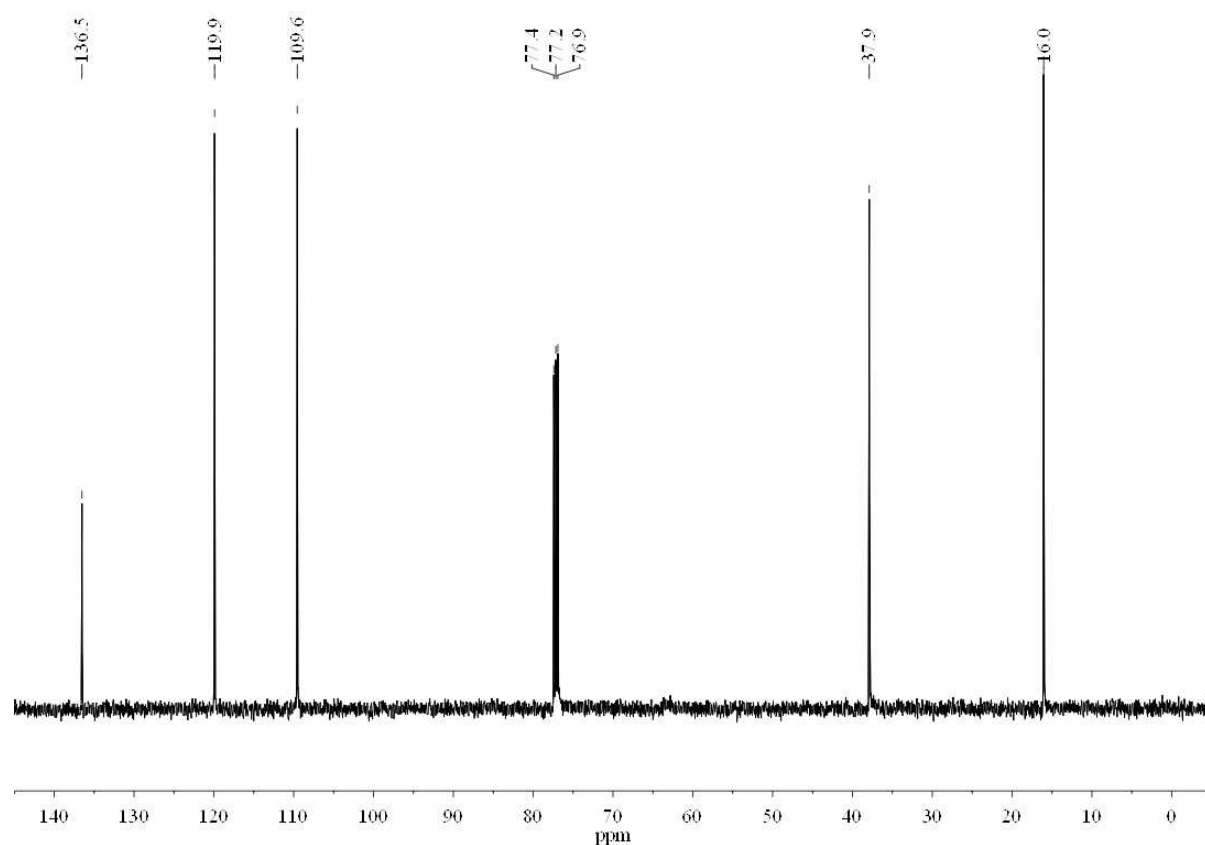


Figure S12: $^{11}\text{B}\{^1\text{H}\}$ NMR spectrum of **18**

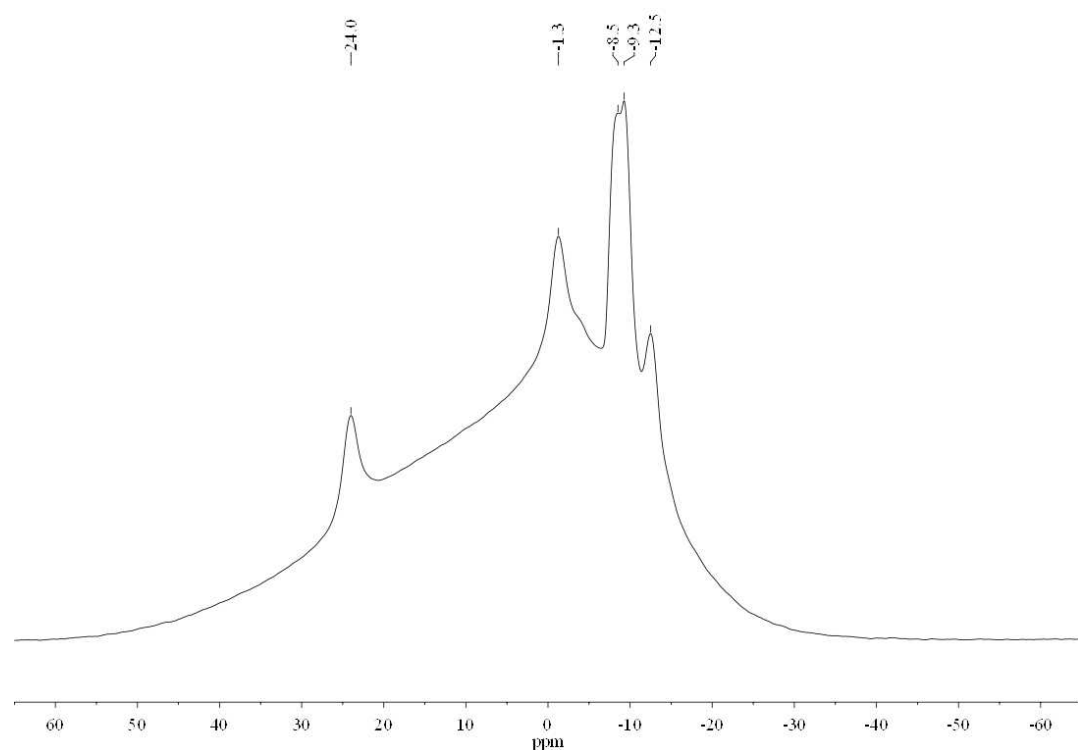


Figure S13: ^1H -NMR spectrum of **19**

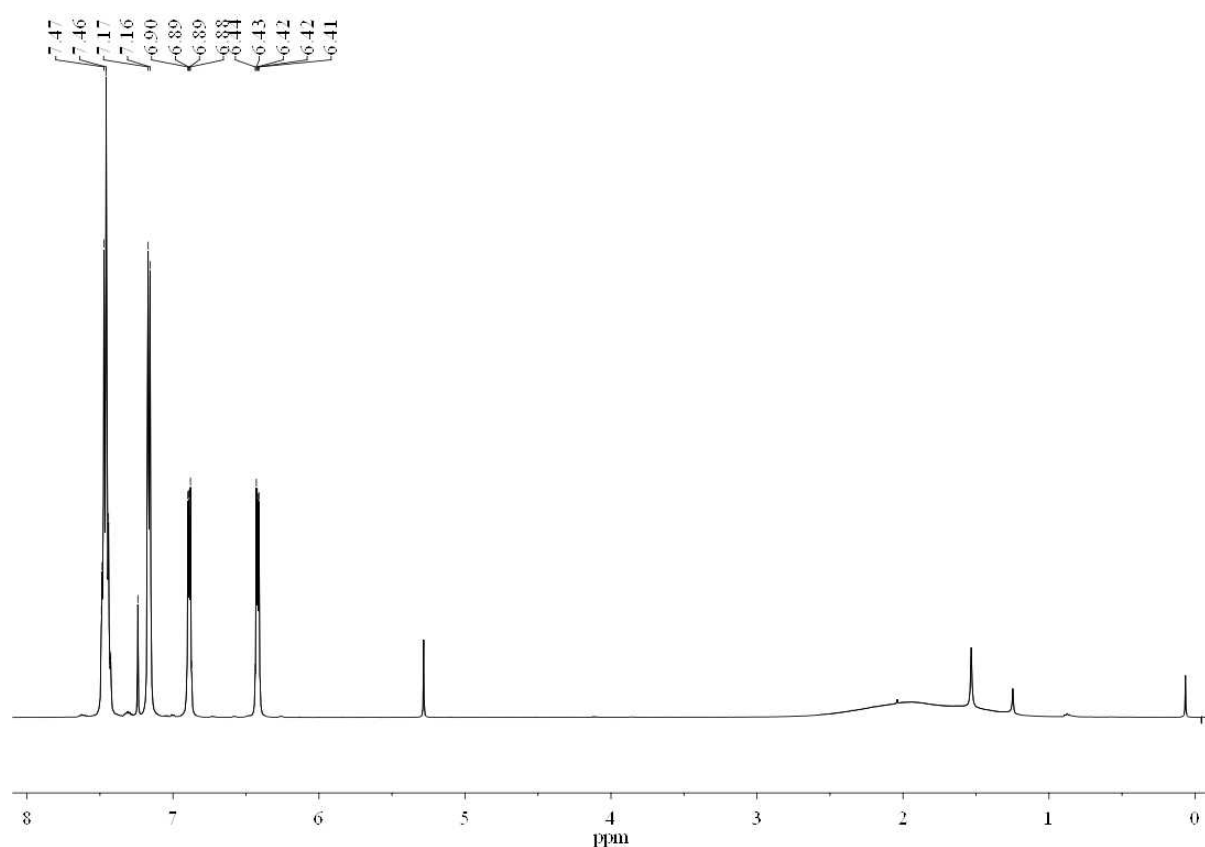


Figure S14: $^1\text{H}\{^{11}\text{B}\}$ NMR spectrum of **19**

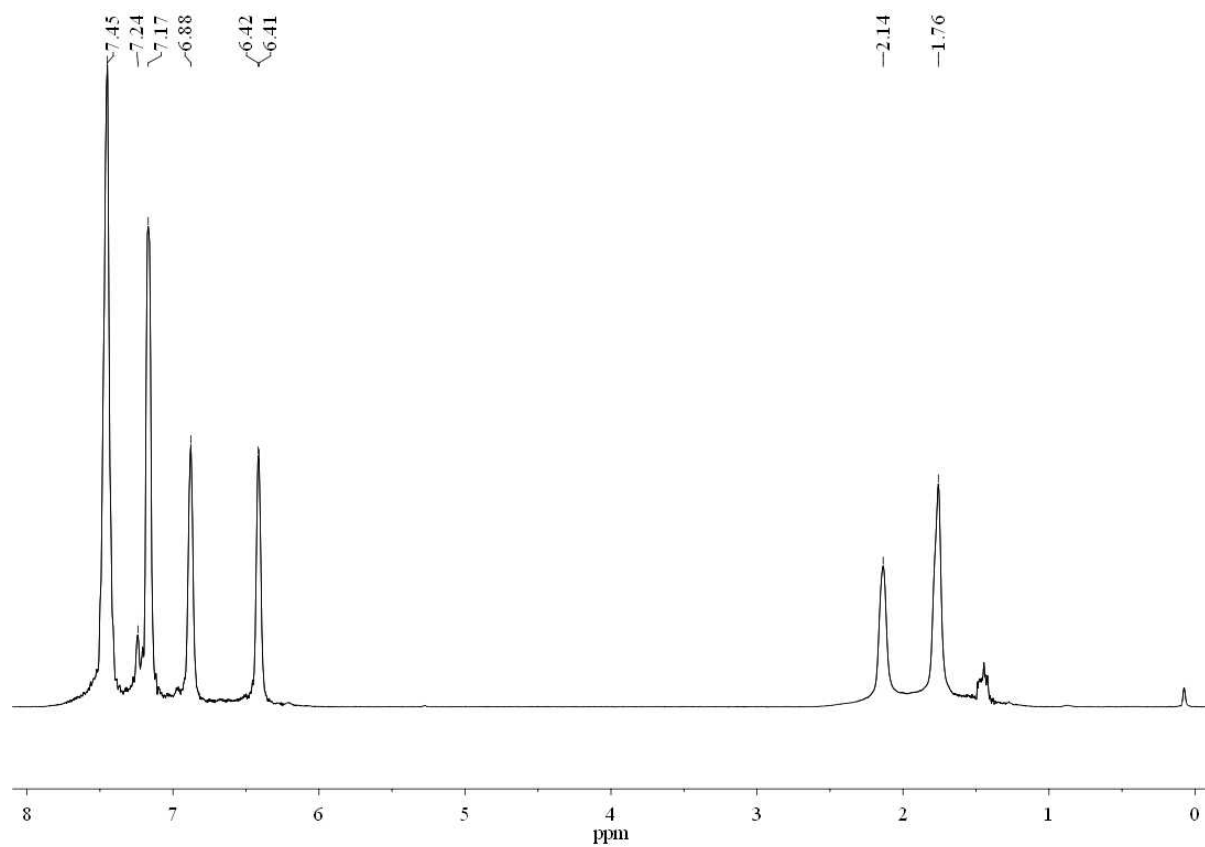


Figure S15: $^{13}\text{C}\{^1\text{H}\}$ NMR spectrum of **19**

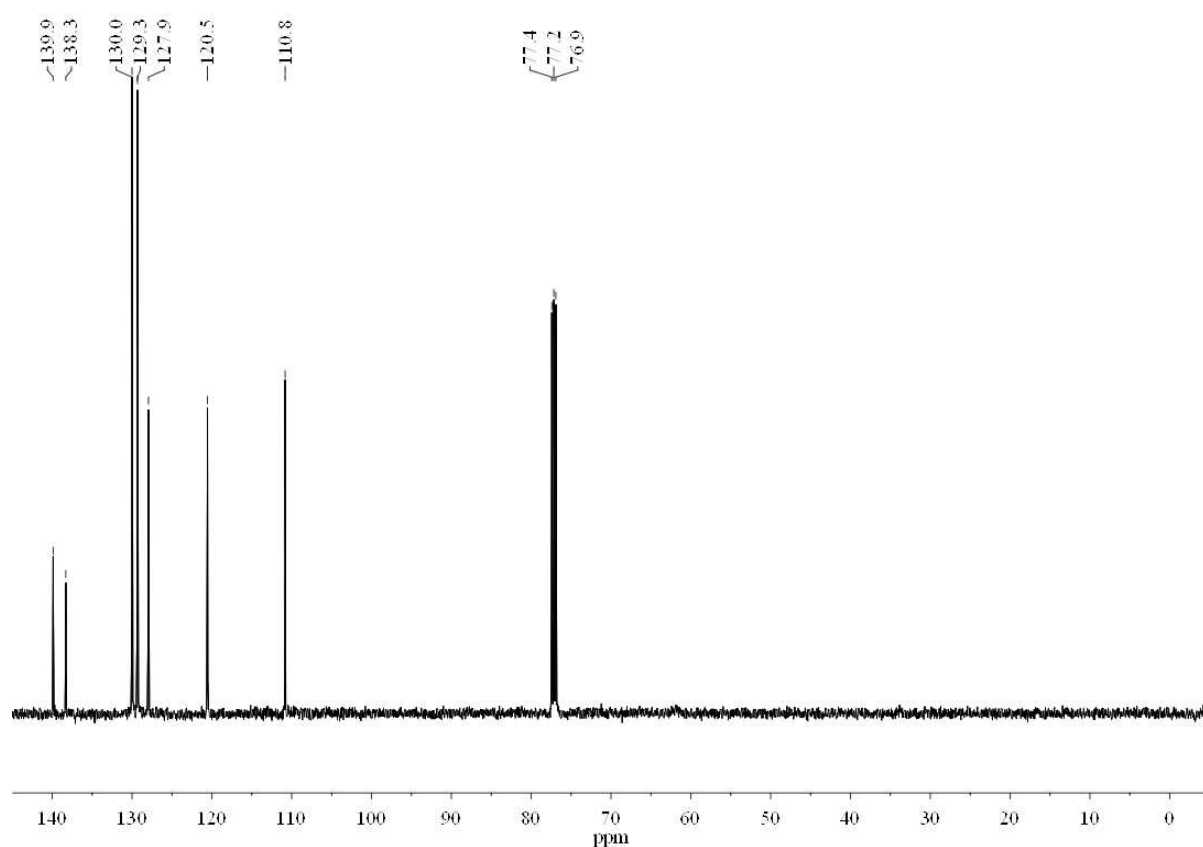


Figure S16: $^{11}\text{B}\{^1\text{H}\}$ -NMR spectrum of **19**

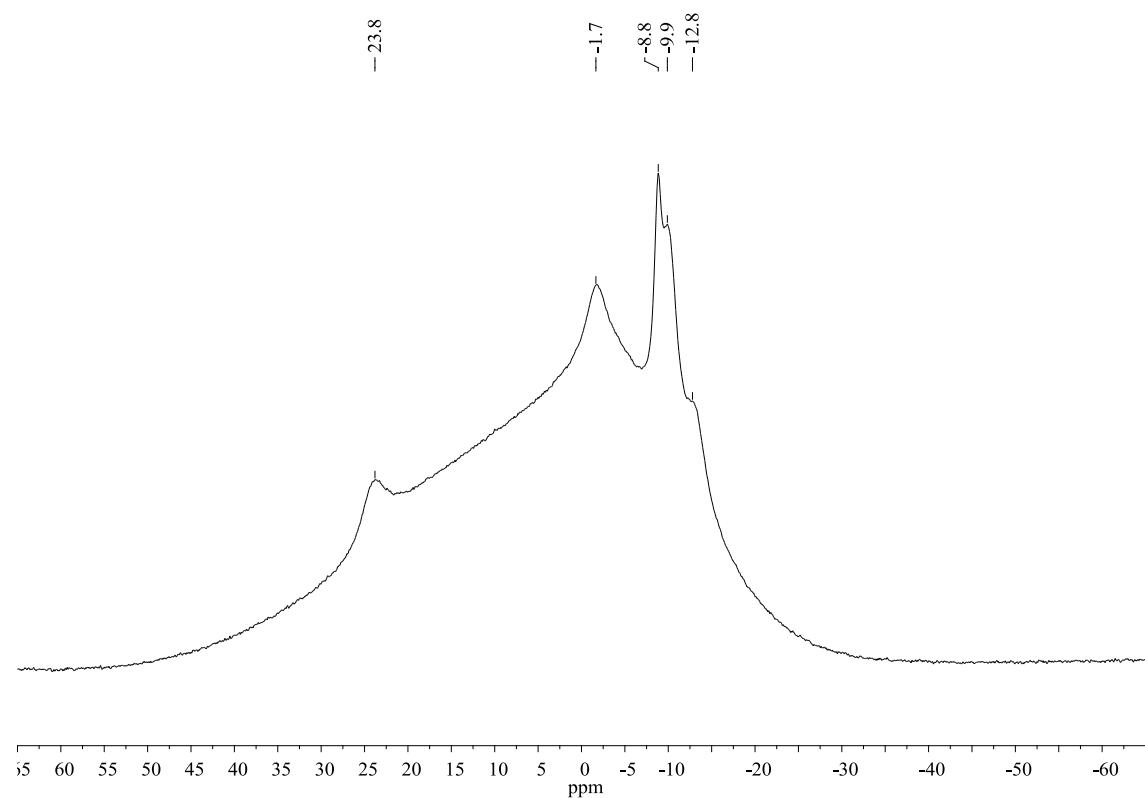


Figure S17: ^1H -NMR spectrum of **20**

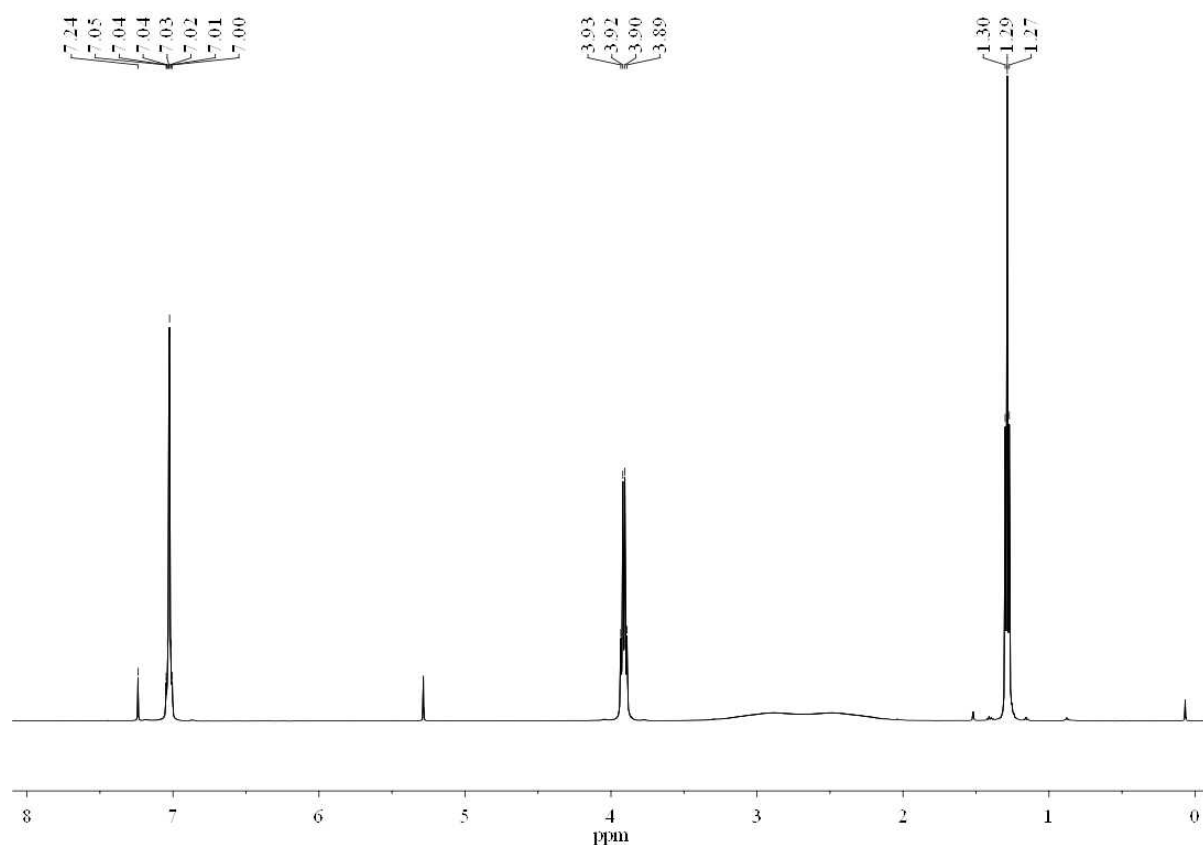


Figure S18: $^1\text{H}\{^{11}\text{B}\}$ -NMR spectrum of **20**

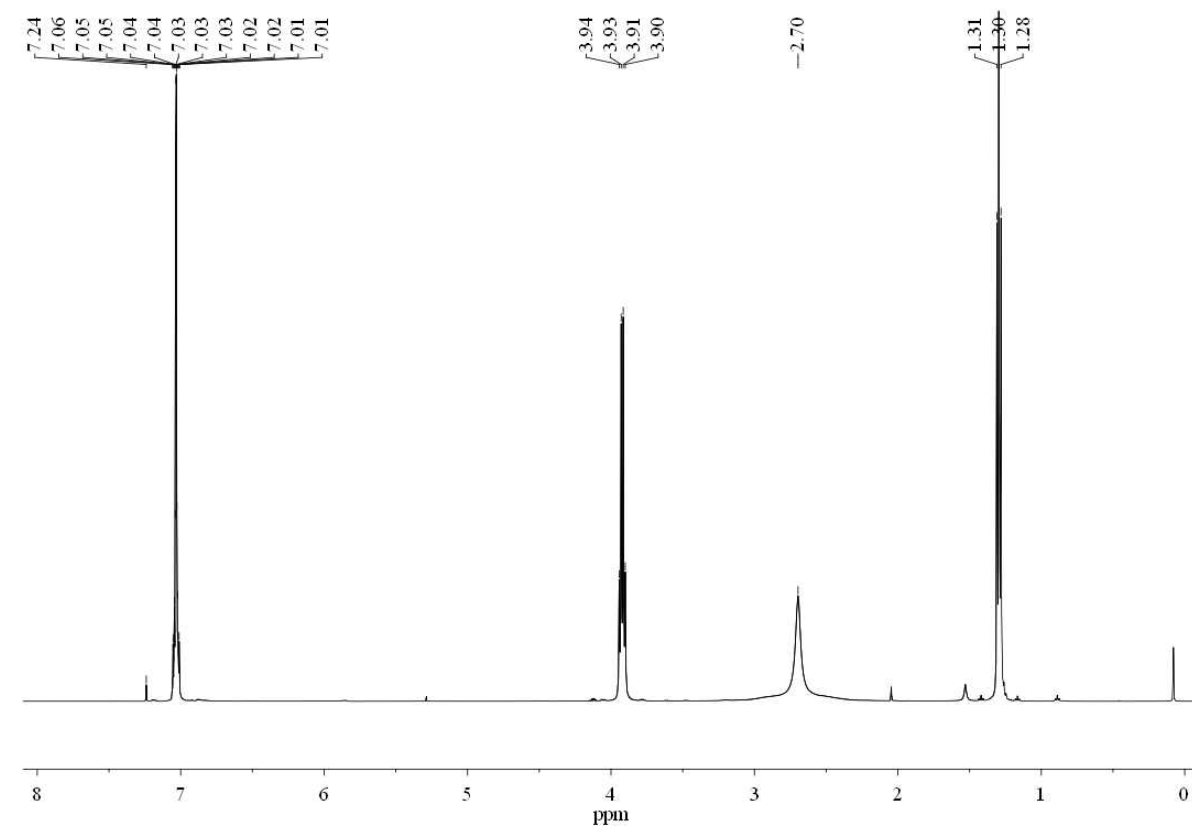


Figure S19: $^{13}\text{C}\{^1\text{H}\}$ -NMR spectrum of **20**

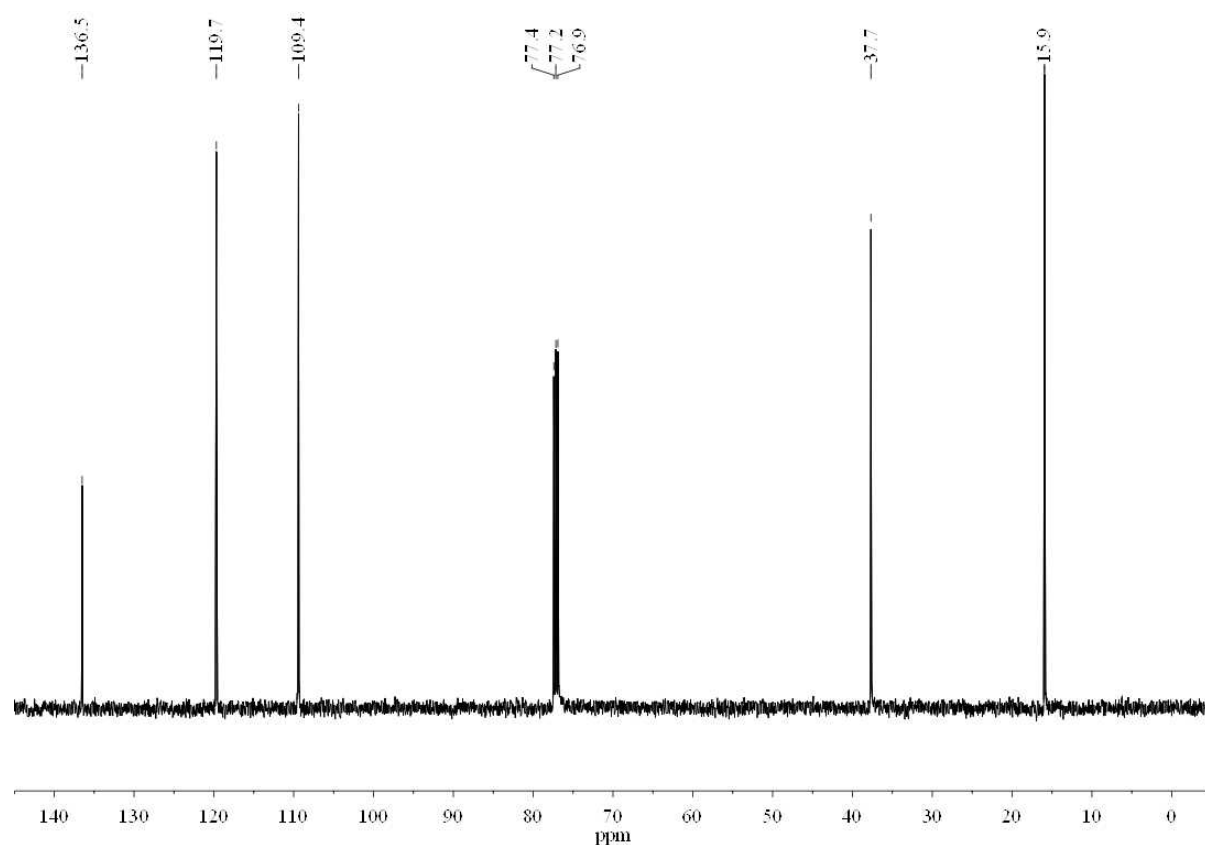


Figure S20: $^{11}\text{B}\{^1\text{H}\}$ -NMR spectrum of **20**

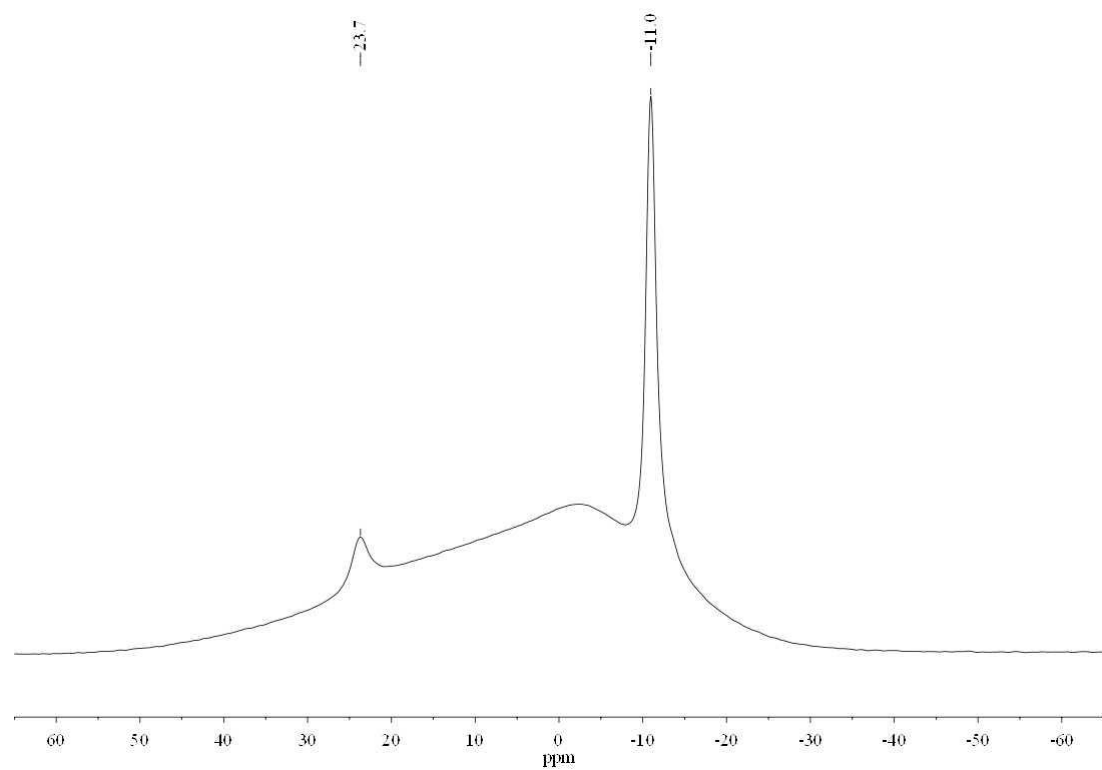


Figure S21: ^1H -NMR spectrum of **21**

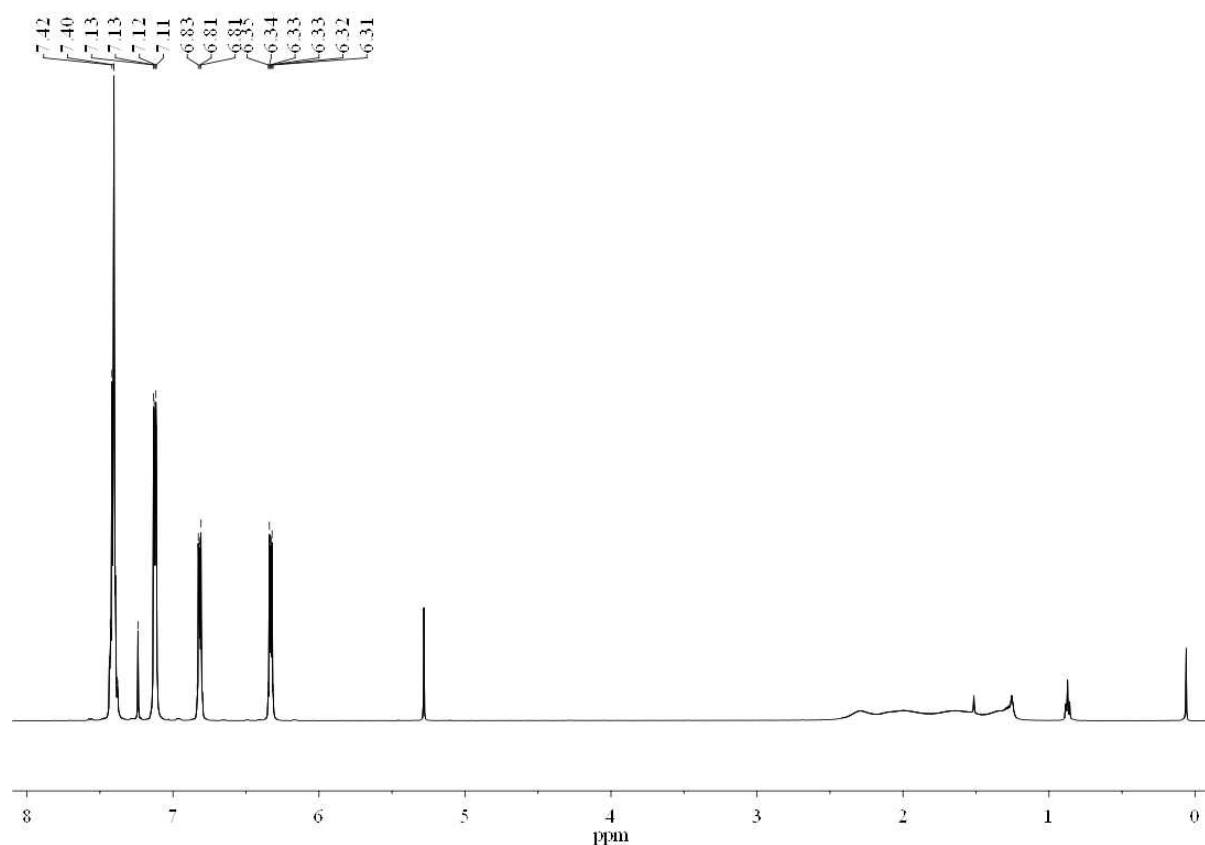


Figure S22: $^1\text{H}\{^{11}\text{B}\}$ -NMR spectrum of **21**

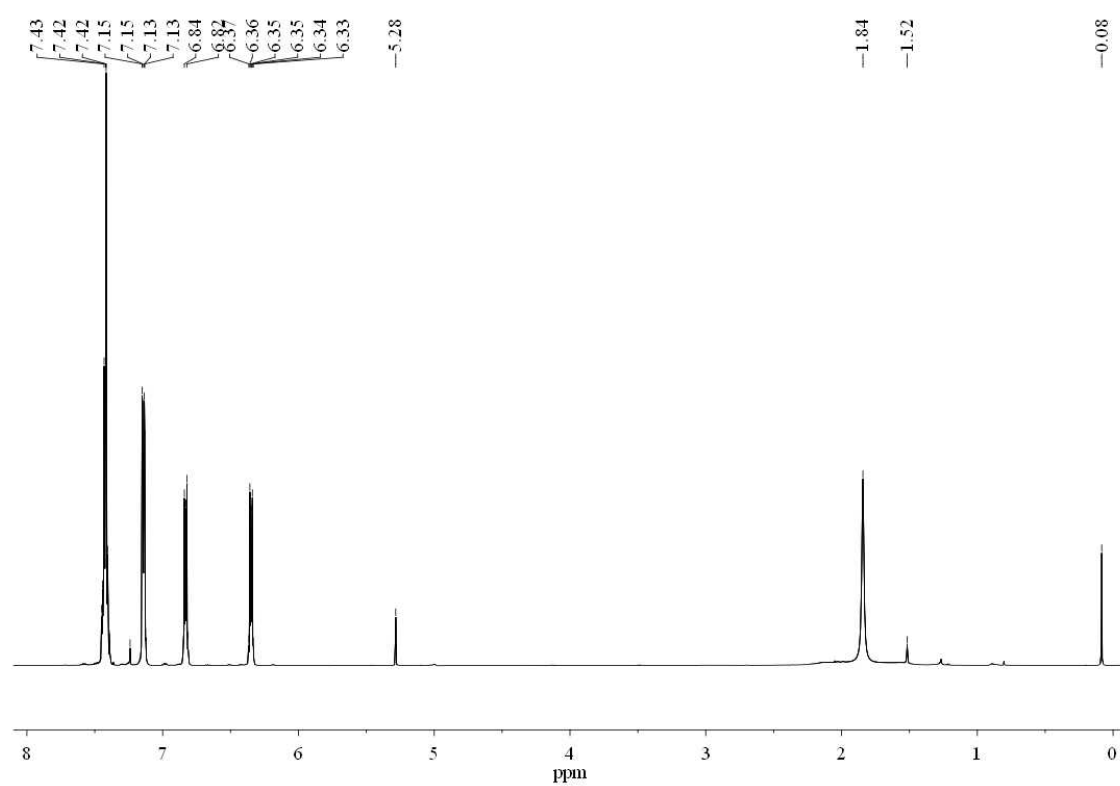


Figure S23: $^{13}\text{C}\{\text{H}\}$ -NMR spectrum of **21**

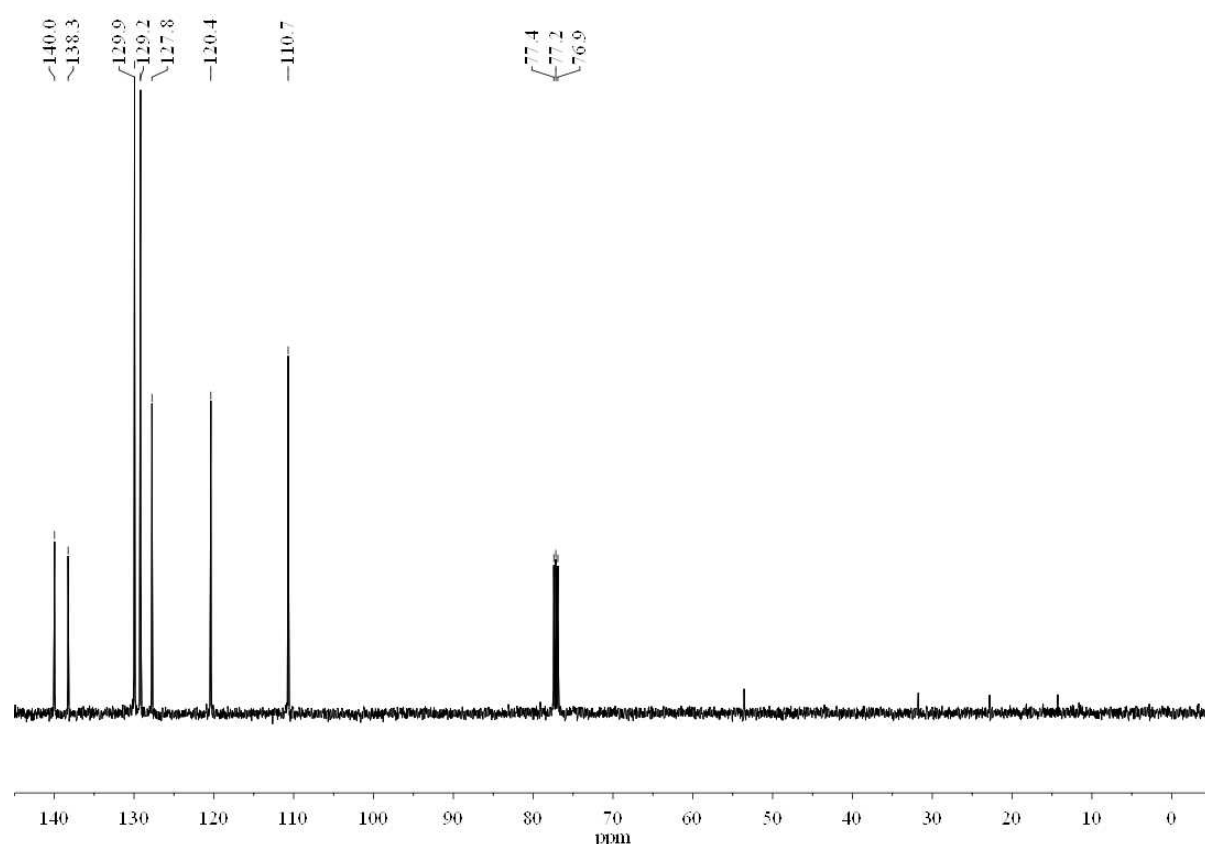


Figure S24: $^{11}\text{B}\{\text{H}\}$ -NMR spectrum of **21**

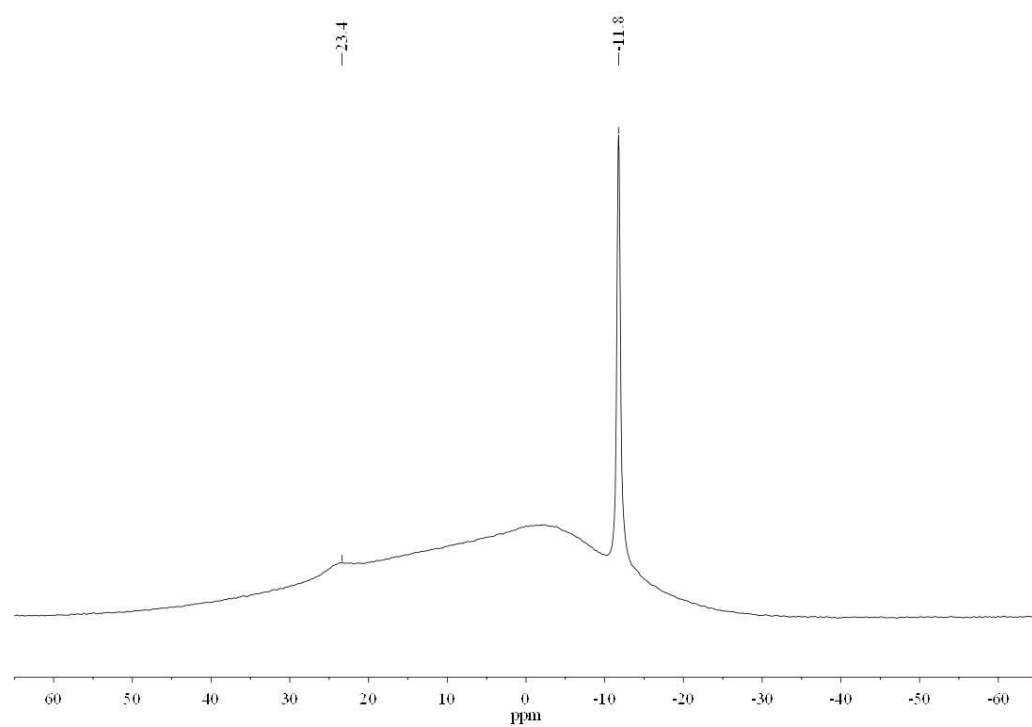


Table S1. Crystallographic data for compounds **16 - 19, 21** and **23**.

compound	16 (CCDC-847434)	17 (CCDC-847435)	18 (CCDC-847436)	19 (CCDC-847437)	21 (CCDC-929985)	23 (CCDC-929986)
diffractometer	Nonius Kappa CCD				Bruker ApexII	
temperature [K]	100	200	100	100	100	100
formula	C ₂₃ H ₄₀ B ₁₂ Cl ₂ N ₄	C ₃₉ H ₄₀ B ₁₂ Cl ₂ N ₄	C ₂₂ H ₃₈ B ₁₂ N ₄	C ₃₈ H ₃₈ B ₁₂ N ₄	3 (C ₃₈ H ₃₈ B ₁₂ N ₄), 4 (CH ₂ Cl ₂)	C ₂₂ H ₂₃ BN ₂
M _r [g mol ⁻¹]	573.21	765.37	488.28	680.44	2381.04	326.23
Crystal system, space group	Monoclinic C2/c	Monoclinic P2 ₁ /c	Monoclinic C2/c	Monoclinic C2/c	Monoclinic C2/c	Trigonal R ³
Unit cell dimensions	a = 34.6741(8) Å b = 9.9071(2) Å c = 19.1591(3) Å β = 111.5852(12)°	a = 11.24370(10) Å b = 21.5876(3) Å c = 16.9579(2) Å β = 102.7367(6)°	a = 17.41830(10) Å b = 8.89920(10) Å c = 17.30630(10) Å β = 91.6578(4)°	a = 17.0270(8) Å b = 11.1965(6) Å c = 19.2084(10) Å β = 100.629(3)°	a = 29.3487(16) Å b = 24.8869(12) Å c = 22.5365(11) Å β = 130.554(3) °	a = 18.3607(6) Å b = 18.3607(6) Å c = 27.8834(11) Å γ = 120 °
Volume [Å ³]	6120.0(2)	4014.81(8)	2681.51(4)	3599.1(3)	12506.7(11)	8140.6(5)
Z, calc. density [Mg/m ³]	8, 1.244	4, 1.266	4, 1.209	4, 1.256	4, 1.265	18, 1.198
Absorption coefficient [mm ⁻¹]	0.236	0.198	0.065	0.069	0.234	0.069
F(000)	2400	1584	1032	1416	4920	3132
Crystal size [mm ³], colour and habit	0.20 x 0.16 x 0.08, Colourless fragment	0.14 x 0.08 x 0.05, Colourless fragment	0.30 x 0.30 x 0.30, Colourless irregular	0.18 x 0.12 x 0.10, Colourless fragment	0.35 x 0.30 x 0.19, Colourless octahedron	0.21 x 0.15 x 0.10, Colourless fragment
θ range [°]	2.97 - 27.49	3.09 - 25.00	3.51 - 30.00	2.91 - 24.99	2.75 - 27.50	2.95 – 30.00
Reflections collected / unique	40700 / 7007 [R(int) = 0.042]	33634 / 7055 [R(int) = 0.059]	67508 / 3906 [R(int) = 0.025]	11323 / 3164 [R(int) = 0.049]	180817 / 14347 [R(int) = 0.034]	64555 / 5272 [R(int) = 0.094]
Data Completeness	99.7%	99.8%	99.4%	99.8%	99.8%	99.9%
Data / restraints / parameters	7007 / 0 / 530	7055 / 1 / 527	3906 / 0 / 194	3164 / 1 / 238	14347 / 8 / 817	5272 / 0 / 229
Goodness-of-fit (F ²)	1.035	1.071	1.042	1.025	1.063	1.009
Final R ₁ , wR ₂ [I>2σ(I)]	0.0405, 0.1000 [5643]	0.0759, 0.2171 [4636]	0.0381, 0.1042 [3675]	0.0499, 0.1110 [2252]	0.0703, 0.1976 [12351]	0.0489, 0.0992 [3323]
R ₁ , wR ₂ (all data)	0.0544, 0.1078	0.1053, 0.2362	0.0397, 0.1056	0.0777, 0.1248	0.0837, 0.2173	0.1024, 0.1238
Largest diff. peak and hole [eÅ ⁻³]	0.525 and -0.795	0.416 and -0.386	0.388 and -0.198	0.209 and -0.189	1.175 and -0.741	0.351 and -0.246

Additional photophysical data

Table S2. Absorption data for **16 – 21**

Compound	Absorption λ_{\max} [nm] (ϵ [$\text{L}\cdot\text{mol}^{-1}\cdot\text{cm}^{-1}$]) in cyclohexane	Absorption λ_{\max} [nm] (ϵ [$\text{L}\cdot\text{mol}^{-1}\cdot\text{cm}^{-1}$]) in DCM	Absorption λ_{\max} [nm] in the solid state
16	289 (16950), 296 (16510)	290 (23030), 296 (22200)	299
17	285 (18830), 292 (19860)	286 (19720), 293 (20210)	287, 294 ^[a]
18	287 (25470), 293 (25300)	288 (19650), 294 (20530)	294, 299 ^[a]
19	284 (11720), 290 (13910)	285 (19980), 291 (22340)	288, 294 ^[a]
20	288 (26900), 291 (26880), 297 (35620)	291 (29350), 297 (36520)	290, 294, 300 ^[a]
21	285 (13640), 291 (17800)	286 (22760), 292 (27730)	288, 295 ^[a]
22	288, 294	288, 294 ^[c, d]	— ^[b]
23	— ^[b]	— ^[b]	289

[a] Global maximum of the spectrum. [b] decomposition. [c] Reference 23. [d] Not recorded in DCM, values are quoted with tetrahydrofuran (THF) which has a similar solvent polarity.

Table S3: Extinction coefficients ($\text{L}\cdot\text{mol}^{-1}\cdot\text{cm}^{-1}$) for **16 - 21** in various solvents (wavelength in brackets)

Compound	CyH	Toluene	CHCl_3	DCM
16	16950 (289), 16510 (296)	21080 (290), 20090 (297)	22420 (291), 21690 (297)	23030 (290), 22200 (296)
17	18830 (285), 19860 (292)	19000(286), 20020 (293)	19690 (286), 20220 (293)	19720 (286), 20210 (293)
18	25470 (287), 25300 (293)	24370 (288), 24870 (295)	25210 (289), 26330 (295)	19650 (288), 20530 (294)
19	11720 (284), 13910 (290)	18470 (285), 22340 (291)	18380 (285), 20210 (291)	19980 (285), 22340 (291)
20	26900 (288), 26880 (291), 35620 (297)	25080 (291), 32700 (298)	25680 (291), 31370 (298)	29350 (291), 36520 (297)
21	13640 (285), 17800 (291)	20430 (286), 26830 (292)	11580 (286), 13500 (292)	22760 (286), 27730 (292)

Table S4: Excitation wavelengths used for emission spectra of **16 - 21** as solids and in various solvents

Compound	Solid	CyH	Toluene	CHCl ₃	DCM
16	350	290	290	290	290
17	310	290	290	290	290
18	306	294	295	-	287
19	275	290	290	-	290
20	275	290	290	-	290
21	280	290	290	-	290

Table S5: Photoluminescence quantum yields in % for compounds **16 - 21** as solids and in various solvents (UV / Vis)

Compound	Solid	CyH	Toluene	CHCl ₃	DCM
16	3	< 1 / 1	< 1	< 1	< 1
17	14	< 1 / 1	1	< 1	< 1
18	< 1	26	< 1 / 2	-	< 1 / 2
19	28	1	2	-	1 / < 1
20	9	41	4 / 2	-	< 1 / < 1
21	72	3	2	-	1

Table S6: Stokes shifts (cm⁻¹) for compounds **16 - 21** as solids and in various solvents (UV / Vis)

Compound	Solid	CyH	Toluene	CHCl ₃	DCM
16	18720	3790 / 18340	20270	20640	21290
17	18200	5520 / 17330	18750	19850	20670
18	13320	1700 / 9830	1900 / 12590	-	2170 / 15170
19	1770	1440	1710	-	1790 / 13210
20	1560 / 8320	1430	1860 / 11390	-	1860 / 12720
21	5980	1450	1720	-	1750

Figure S25: Absorption spectra for **16 - 21**

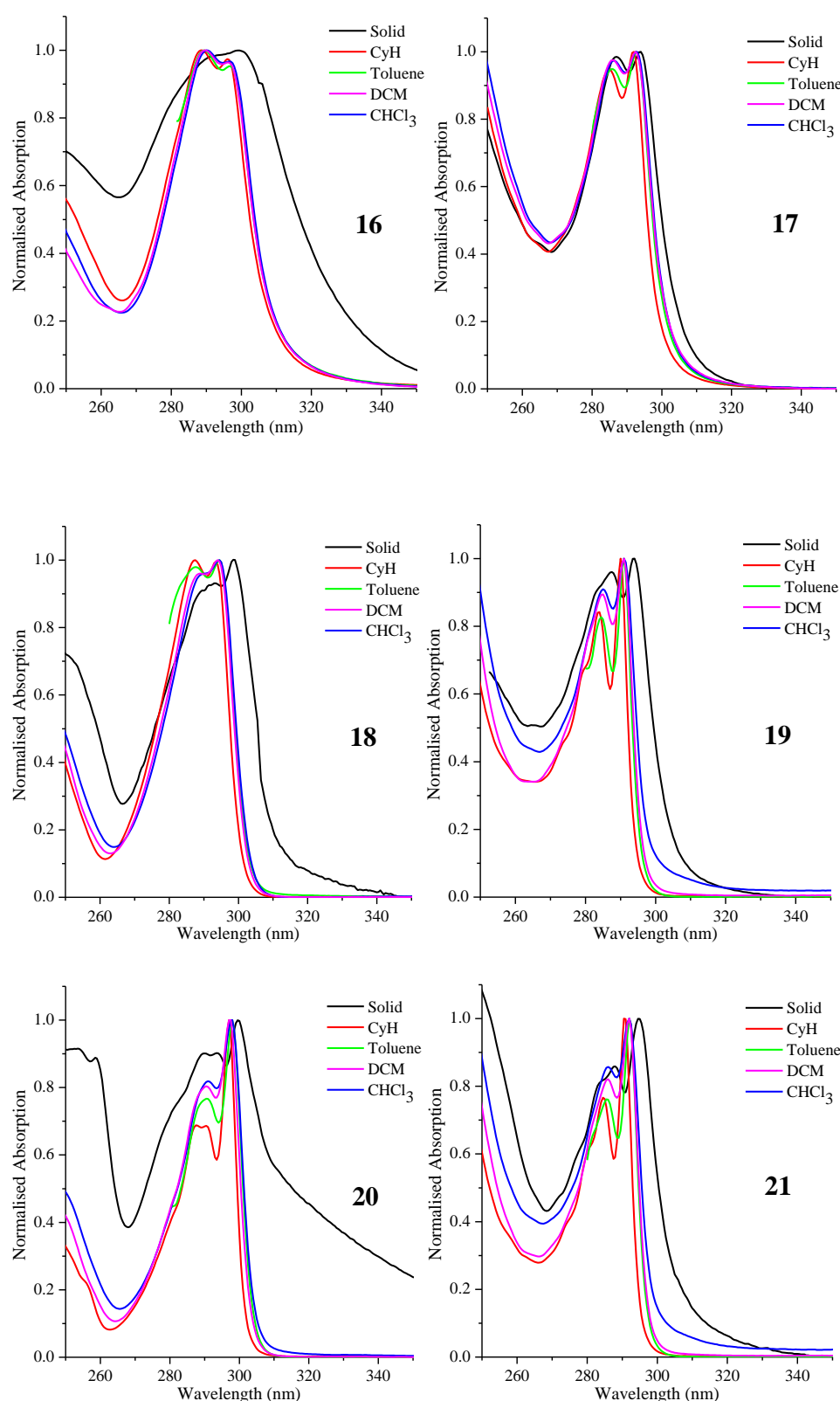
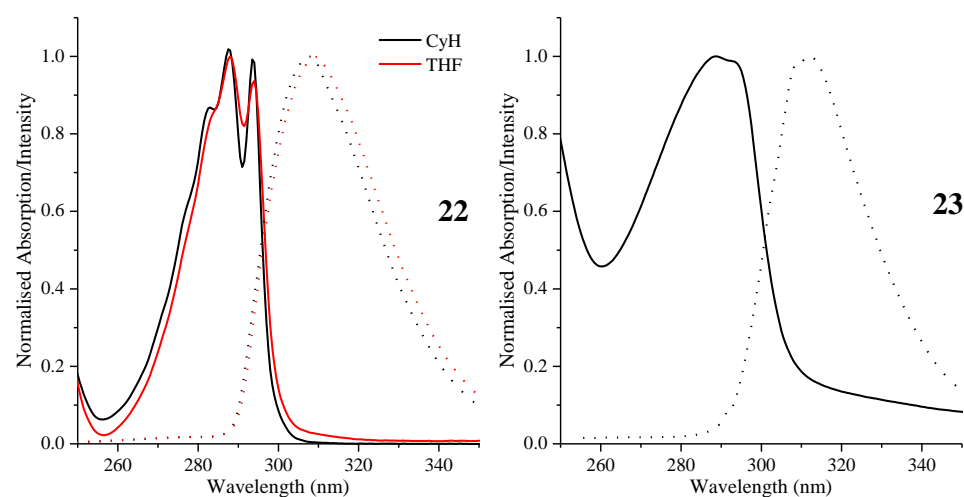
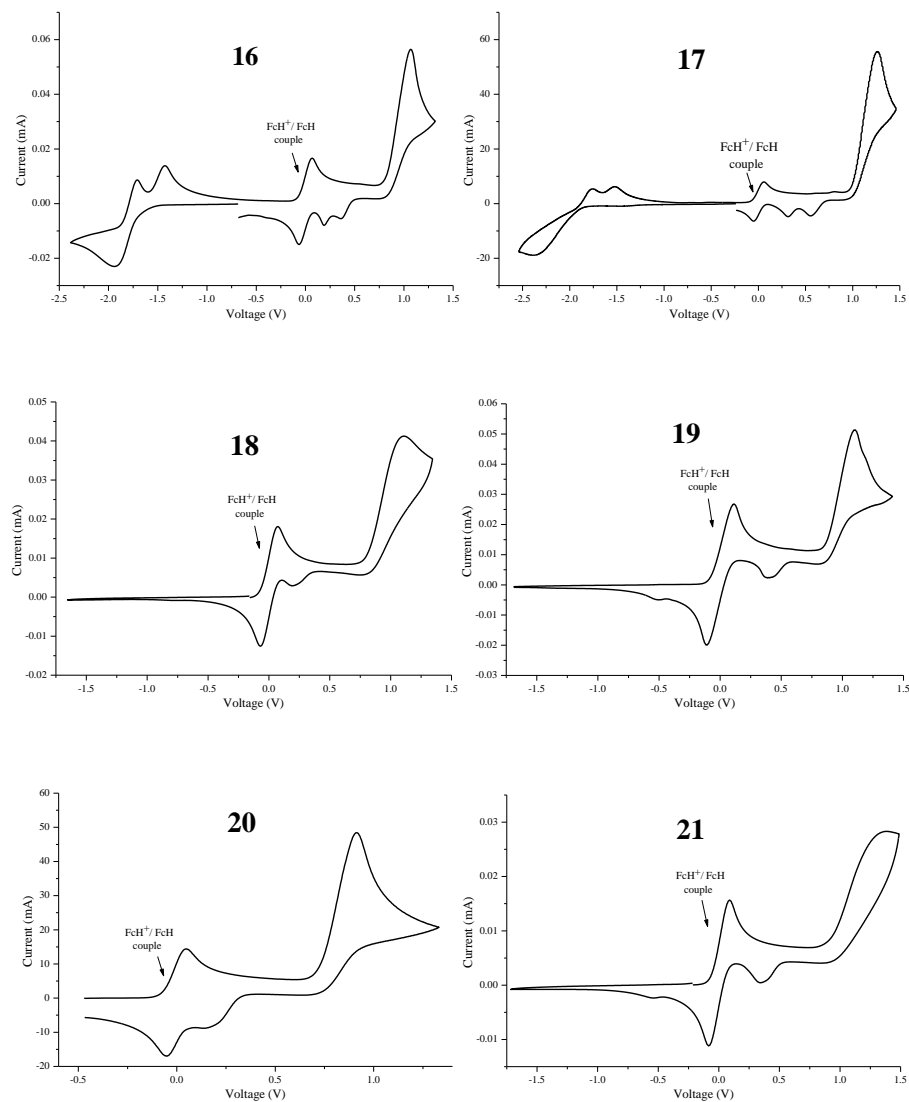


Figure S26: Absorption (solid line) and emission (dashed line) spectra for **22** (left) in cyclohexane and THF and **23** (right) in the solid state.



Additional electrochemical data

Figure S27: Cyclic voltammograms of **16 - 21** in dichloromethane.



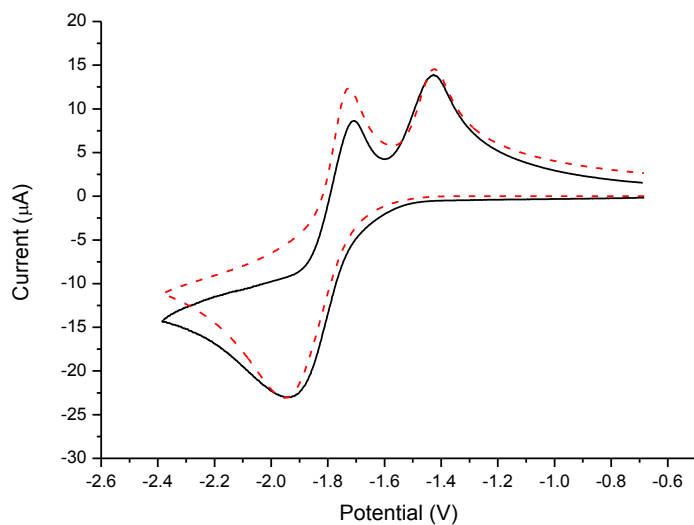


Figure S28: Experimental (black solid line) and simulated (red dashed line, Redox(0/-1): $E^\circ = -1.590$ V, $k^\circ = 2.0 \times 10^{-4}$ cm/s, $\alpha = 0.34$; Redox(-1/-2): $E^\circ = -1.790$ V, $k^\circ = 2.0 \times 10^{-3}$ cm/s, $\alpha = 0.30$) CV of **16** in dichloromethane.

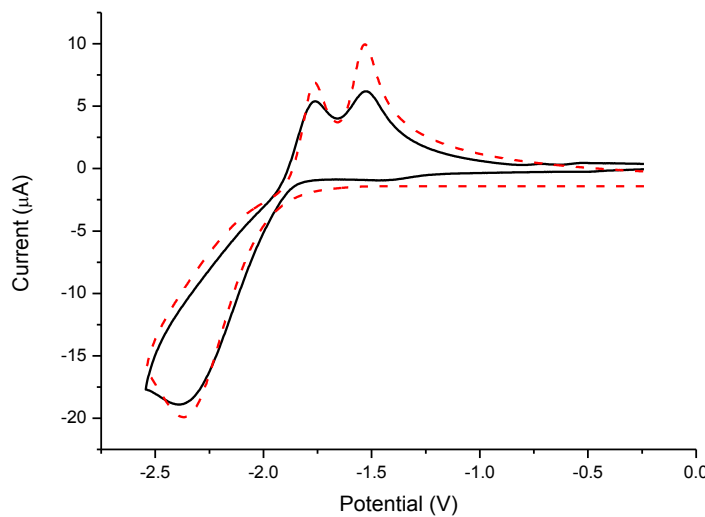


Figure S29: Experimental (black solid line) and simulated (red dashed line, Redox(0/-1): $E^\circ = -1.720$ V, $k^\circ = 1.5 \times 10^{-5}$ cm/s, $\alpha = 0.22$; Redox(-1/-2): $E^\circ = -1.890$ V, $k^\circ = 1.0 \times 10^{-4}$ cm/s, $\alpha = 0.20$) CV of **17** in dichloromethane.

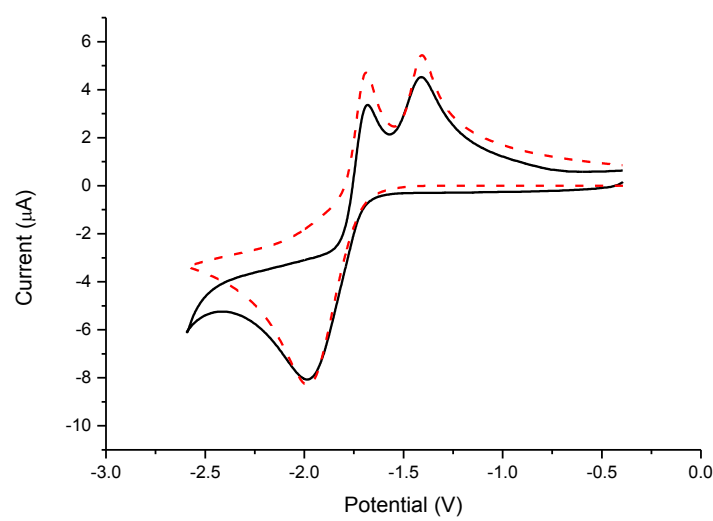


Figure S30: Experimental (black solid line) and simulated (red dashed line, Redox(0/-1): $E^\circ = -1.583$ V, $k^\circ = 2.5 \times 10^{-3}$ cm/s, $\alpha = 0.30$; Redox(-1/-2): $E^\circ = -1.743$ V, $k^\circ = 1.0 \times 10^{-3}$ cm/s, $\alpha = 0.20$) CV of diphenyl-*ortho*-carborane **24** in dichloromethane.

Additional Computational Data

GIAO-NMR data

GIAO-NMR computations have shown to be an excellent tool in determining the likely geometries of new carboranes based on observed NMR data. The agreements between observed and computed boron NMR peaks have been very good and this method is considered reliable enough to assign the observed ^{11}B peaks to specific boron cluster atoms in carboranes. Table S7 lists the boron peak assignments of observed peaks for **16 - 21**.

Table S7. Comparison between observed and calculated ^{11}B NMR data and assignments of boron peaks.

	$^{11}\text{B}(\text{calc})$	Assignment	$^{11}\text{B}(\text{obs})$	Integrals
16	21.8	B2',2"	22.9	2
	2.8	B9,12	2.5	2
	-4.9	B8,10	-5.2	2
	-8.5	B4,5,7,11	-8.4	4
	-10.2	B3,6	-8.9	2
17	22.5	B2',2"	22.7	2
	2.6	B9,12	0.9	2
	-4.9	B8,10	-6.3	2
	-9.2	B4,5,7,11	-9.6	6
	-10.8	B3,6		
18	23.0	B2',2"	24.0	2
	-0.5	B5,12	-1.3	2
	-7.5	B9,10	-8.5	2
	-8.6	B4,6,8,11	-9.3	4
	-11.5	B2,3	-12.5	2
19	23.2	B2' B2"	23.8	2
	-0.8	B5,12	-1.7	2
	-8.5	B9,10	-8.8	2
	-9.5	B4,6,8,11	-9.9	4
	-12.0	B2,3	-12.8	2
20	22.7	B2',2"	23.7	2
	-10.2	B2-11	-11.0	10
21	22.7	B2',2"	23.4	2
	-11.0	B2-11	-11.8	10

TD-DFT data

Table S8. Comparison of observed and calculated absorption data for bis(benzodiazaborolyl)-carboranes **16 - 21**.

n	Abs (obs)		Abs (calc)		Osc. Strength (f)	Major MO contributions (%)	Transition type $S_0 > S_n$
	in S_n	$S_0 > S_n$ (eV)	$S_0 > S_n$ (eV)	(f)			
16	1	4.19	4.29	0.1145	HOMO-1 > LUMO (47) HOMO > LUMO (50)		$\pi(\text{borolyl}) > \pi\text{B}^*$ $\pi(\text{borolyl}) > \pi\text{B}^*$
17	1	4.25	4.51	0.0940	HOMO-1 > LUMO (68)		$\pi(\text{borolyl}) > \pi\text{B}^*$
18	1	4.23	4.67	0.4126	HOMO-1 > LUMO (58) HOMO > LUMO+1 (35)		$\pi(\text{borolyl}) > \pi\text{B}^*$ $\pi(\text{borolyl}) > \pi\text{B}^*$
19	7	4.28	4.76	0.2720	HOMO-1 > LUMO+2 (30) HOMO-1 > LUMO+3 (29) HOMO > LUMO+9 (27)		$\pi(\text{borolyl}) > \pi^*(\text{phenyl})$ $\pi(\text{borolyl}) > \pi^*(\text{phenyl})$ $\pi(\text{borolyl}) > \pi\text{B}^*$
20	1	4.18	4.51	0.4849	HOMO > LUMO (68)		$\pi(\text{borolyl}) > \pi\text{B}^*$
21	3	4.26	4.72	0.4575	HOMO > LUMO (61)		$\pi(\text{borolyl}) > \pi\text{B}^*$
22	1	4.22	4.88	0.1139	HOMO > LUMO (63)		$\pi(\text{borolyl}) > \pi^*(\text{borolyl})$
23	2	4.23	5.10	0.1079	HOMO-1 > LUMO+1 (47) HOMO > LUMO+4 (45)		$\pi(\text{borolyl}) > \pi^*(\text{phenyl})$ $\pi(\text{borolyl}) > \pi^*(\text{borolyl})$